

# Electronic and Optical Properties of CuO Based on DFT+U and GW Approximation

F Ahmad<sup>1,2,a</sup>, M K Agusta<sup>1,b</sup>, and H K Dipojono<sup>1,c\*</sup>

<sup>1</sup>Laboratory of Computational Material Design & Quantum Engineering, Department of Engineering Physics, Faculty of Industrial Technology, Institut Teknologi Bandung, Bandung, Indonesia.

<sup>2</sup>Department of Physics, Bogor Agricultural University, Bogor, Indonesia.

<sup>a</sup> faozan@apps.ipb.ac.id, <sup>b</sup> kemal@tf.itb.ac.id, <sup>c</sup> dipojono@tf.itb.ac.id

**Abstract.** We report ab initio calculations of electronic structure and optical properties of monoclinic CuO based on DFT+U and GW approximation. CuO is an antiferromagnetic material with strong electron correlations. Our calculation shows that DFT+U and GW approximation sufficiently reliable to investigate the material properties of CuO. The calculated band gap of DFT+U for reasonable value of U slightly underestimates. The use of GW approximation requires adjustment of U value to get realistic result. Hybridization Cu 3d<sub>xz</sub>, 3d<sub>yz</sub> with O 2p plays an important role in the formation of band gap. The calculated optical properties based on DFT+U and GW corrections by solving Bethe-Salpeter are in good agreement with the calculated electronic properties and the experimental result.

## 1. Introduction

Cupric oxide or tenorite (CuO) has attracted attention because of its interesting properties as a p-type semiconductor with a narrow band gap (1.34-1.67 eV) and hence it can be used for fabrication of p-n heterojunctions with other n-type metal oxides such as ZnO and TiO<sub>2</sub>. CuO has been used as an effective modifier of photocatalyst TiO<sub>2</sub> or ZnO in water splitting and CO<sub>2</sub> reduction system [1]. Furthermore, CuO are extensively used in various other applications, including high-temperature superconductors, giant magneto resistance materials, gas sensors, bio-sensors, photodetectors and magnetic storage media [2]. Due to the extensive functions it is important to know the internal properties of CuO theoretically. But conventional computation approach often fail to give accurate result, it is suspected because of the strong electron correlation effects arising from hybridization Cu 3d and O 2p orbital.

The crystal structure of CuO is monoclinic with C2/c symmetry and with four formula units per unit cell. CuO exhibits two antiferromagnetic orderings with different Neel temperatures; those are 213 K and 231K. Below 213 K, CuO exhibits collinear magnetic ordering, between 213 K and 231 K, CuO exhibits a helical magnetic ordering, and at the higher temperatures the system becomes paramagnetic. In this magnetic structure, each O atom is surrounded by a slightly distorted tetrahedron of four Cu atoms and each atom Cu is surrounded by square planar of four ligands of O atoms [2, 3].

Theoretically, the electronic structure of CuO has been studied using either a standard DFT (density functional theory) and DFT+U. Standard DFT failed to predict semiconducting properties of CuO, it is detected as metallic. Calculations by adding a correction factor to the strong electron-electron interactions, namely DFT+U (density functional theory with Hubbard potential (U)



correction), has overcome these problems successfully, although with bandgap value that is still below from the experimental results [4, 5]. Another method used to predict the electronic structure is the GW approximation, it provide corrections to the DFT calculation by taking into account the screening effect through quasi-particle approach. GW approximation is method to solve many-body perturbative (MBP) problem based on Green's function (G) and screened Coulomb's potential (W). GW approximation has successfully predicted bandgap and DOS of semiconductor material with weak electron correlations, while for systems with strong electron correlations as well as CuO, GW approach is not entirely accurate [3, 6].

In this paper we will compare the DFT+U and DFT+U+GW approach to examine the electronic and optical properties of CuO. This article is organized as follows. After this introduction in section 1, method and computational details are given in section 2. The results and discussions of the work are presented in section 3; consist of results and discussions of electronic properties and optical properties of CuO. This article will be concluded in section 4.

## 2. Method and Computational Details

Due to the failure of standard DFT in predicting the material properties of strong electron correlation system, then in this study we used DFT plus effective Coulomb interaction (U) (DFT+U) and the GW correction. Calculations based on DFT and GW approximation were done through Quantum Espresso [7] and Yambo [8] package, respectively. Exchange-correlation term was expressed by using generalized gradient approximation (GGA) based on Perdew–Burke–Ernzerhoff (PBE) functional. Energy cut-off for the expansion of plane-wave basis sets was set at 500 eV. Ion cores were represented by non-conserving (NC) pseudo potential. The integration of the Brillouin zone was done on  $4 \times 4 \times 4$  k-points grid sampled by Monkhorst–Pack scheme.

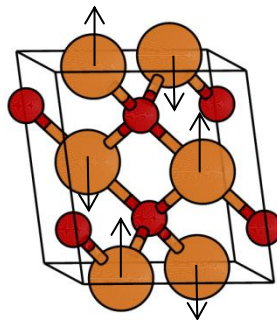


**Figure 1.** Bulk structure and antiferromagnetic spin ordering of bulk CuO.

The lattice parameters of CuO are  $a = 4.690 \text{ \AA}$ ,  $b = 3.420 \text{ \AA}$ ,  $c = 5.131 \text{ \AA}$  and  $\beta = 99.540^\circ$  [9]. Figure 1 shows the bulk structure and the antiferromagnetic spin ordering of CuO, arrow up on Cu atom indicate majority spin direction and arrow down indicate minority spin direction.

## 3. Results and Discussions

The calculation begins with band structure of CuO calculated using spin polarized and non-polarized DFT. It aims to demonstrate the problems in the calculation of CuO as a strong electron correlation material. In figure 2(a), we show the calculated band structure of CuO within non-spin-polarized approach, it appears that the DFT fail to predict the insulator properties of CuO and on the other hand in figure 2(b), the spin-polarized approach with enabled AFM has proven the semiconductor properties of CuO with very small band gap (still tend to be conductor), but this result is still far from the experiment results. Based on the problem, another approach is needed to be able to investigate the properties of CuO reliably. Here we have used DFT+U and GW approximation to resolve the band gap of CuO. The calculated bandgap based on DFT+U and GW approximation are shown in Table 1. Some of the results are in line with experiment.

Another important parameter to be considered in the calculation of magnetic material is local or atomic magnetic moments. In Table 1, we show the calculated atomic magnetic moment and the band gap of CuO within DFT+U, and GW method. The calculated magnetic moment per Cu atom ( $\mu$ -Cu) for  $U = 1 - 3$  eV are  $6.7 - 7.4 \mu_B$ , in good agreement with the experimental result, but the magnetic moment per O atom slightly out of the range of the experimental data. The band gap and the atomic magnetic moments become a reference that shows the calculation and the model relevant or not to the actual material.

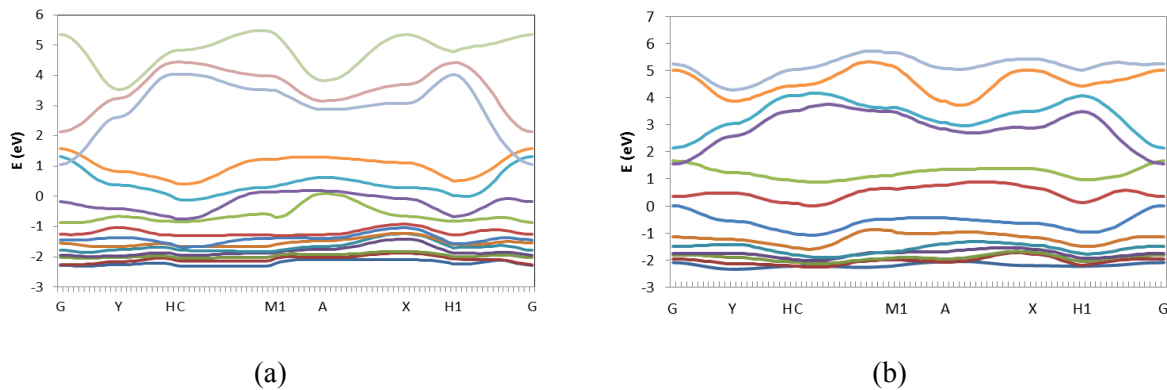


**Figure 2.** Band structure of CuO calculated with non-polarized DFT (a), and spin-polarized-AFM DFT (b).

**Table 1.** Band gap and local magnetic moment of CuO calculated in various method calculations and experimental data.

Method	$\mu$ -Cu ( $\mu_B$ )	$\mu$ -O ( $\mu_B$ )	Direct band gap (eV)	Indirect band gap (eV)
DFT	0.61	0.0598	0.35	0.006
DFT+U, U=1	0.67	0.0593	0.63	0.38
DFT+U, U=2	0.71	0.0556	1.05	0.84
DFT+U, U=3	0.74	0.0514	1.66	1.41
DFT+U, U=4	0.76	0.0468	2.10	1.69
DFT+G <sub>0</sub> W <sub>0</sub>			0.76	1.73
DFT+U+G <sub>0</sub> W <sub>0</sub> , U=0.1			0.97	1.96
DFT+U+G <sub>0</sub> W <sub>0</sub> , U=0.3			1.54	2.37
DFT+U+G <sub>0</sub> W <sub>0</sub> , U=0.35			1.69	2.47
Exp.	$0.65 \pm 0.03$ [10]	$0.14 \pm 0.04$ [10]	1.34 (300K) [12]	
	$0.69 \pm 0.05$ [11]		1.67 (0K) [12]	

### 3.1. Electronic Properties

The discussion of electronic properties begins with DFT+U method. The Hubbard potential ( $U$ ) in this calculation is applied simultaneously to the Cu  $3d$  and O  $2p$  state, instead of to Cu  $3d$  like previous studies [3, 4, 5]. By applying  $U$  to two orbital simultaneously, the shifting of calculated band gap become larger for the same value of  $U$ . In this calculation, the value of  $U$  is varied between 0.0 to 4.0 eV. At  $U = 0.0$  eV (pure DFT), CuO tends to be detected as a conductor (metallic properties), as shown by the overlapping bands around the Fermi level (see figure 3 and 4). By applying  $U$ , the Coulomb interaction between electrons in the orbital Cu  $3d$  and O  $2p$  are corrected by the effective potential (Coulomb screening), so that the bandgap CuO could be formed. From Table 1, we can interpolate that the calculated band gap of DFT+U increase linearly with  $U$ . The realistic values of  $U$

that can be accepted are confirmed by the appropriate bandgap and atomic magnetic moment which is consistent with experimental data. For  $U = 3$ , we find band gap  $E_g = 1.41$  close to the experiment result at room temperature, but DFT calculation is conducted in zero temperature. Therefore, even though DFT+U are able to open the bandgap CuO but the results are still under expectation.

From figure 3, it appears that the formation of the CuO bandgap dominated by orbital Cu  $3d_{xz}$ ,  $3d_{yz}$  and O  $2p$ , it is different with the previous results [3, 5] where the band gap dominated by  $3d_{x^2-y^2}$ . Here hybridization Cu  $3d_{xz}$ ,  $3d_{yz}$  with O  $2p$  plays an important role in the formation of CuO bandgap. Unoccupied Cu  $3d_{xz}$  and  $3d_{yz}$  contribute to the formation of CBM while hybridization Cu  $3d_{xz}$  and  $3d_{yz}$  in opposite spin with O  $2p$  contribute to the VBM formation. Figure 4 shows that orbital Cu  $3d_{x^2-y^2}$ ,  $3d_{z^2}$ , and  $3d_{xy}$  hybridized with O  $2p$  weakly, so that it has fewer roles in the formation of the band gap.

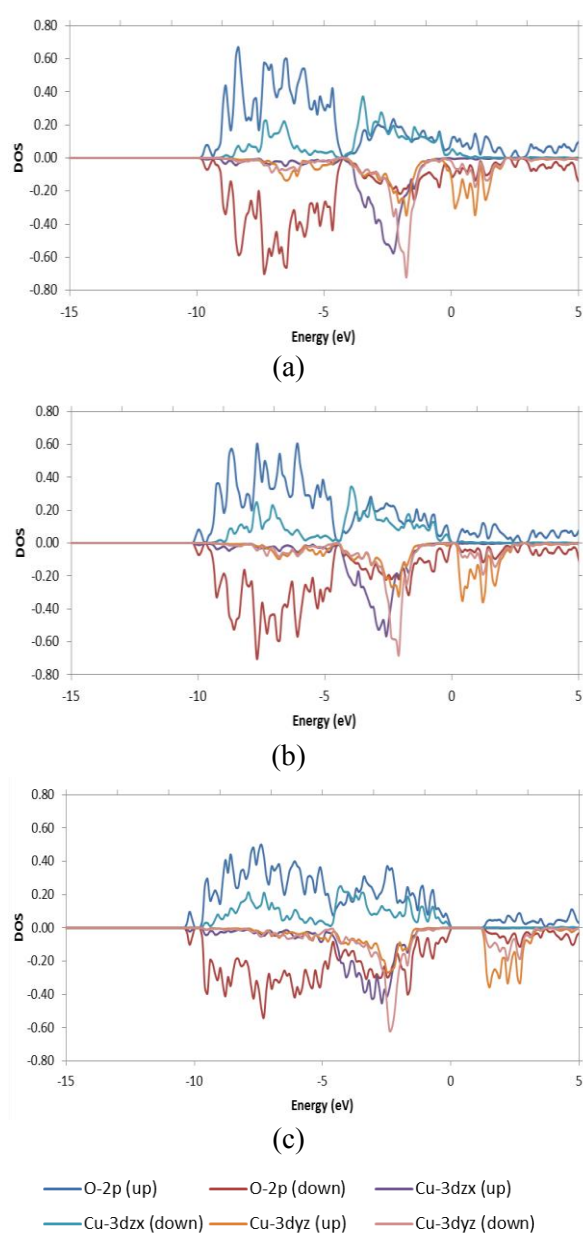


**Figure 3.** Projected DOS (PDOS) of Cu $3d_{xz}$ ,  $3d_{yz}$ , and O $2p$  orbital calculated with DFT+U;  $U = 0$  eV (a),  $U = 1$  eV (b),  $U = 3$  eV (c).

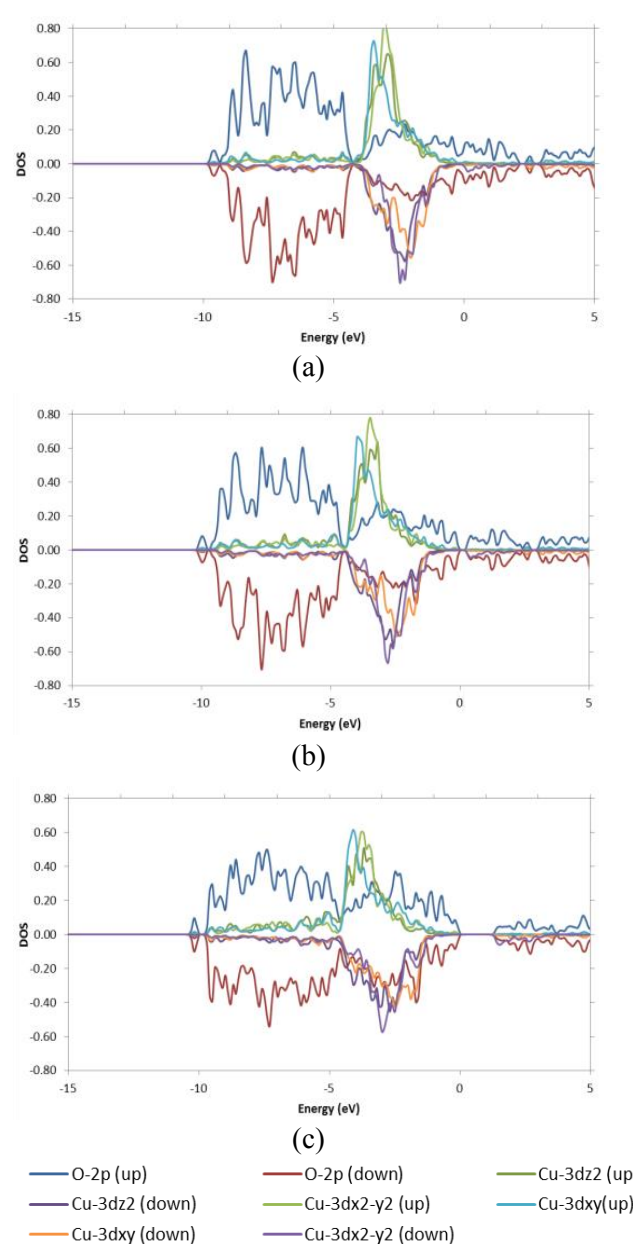


**Figure 4.** Projected DOS (PDOS) of Cu $3d_{x^2-y^2}$ ,  $3d_{z^2}$ ,  $3d_{xy}$  and O $2p$  orbital calculated with DFT+U;  $U = 0$  eV (a),  $U = 1$  eV (b),  $U = 3$  eV (c).

By analyze the PDOS peaks of orbital Cu  $3d$  can be concluded that the orbital  $3d_{xz}$  and  $3d_{yz}$  occupy the highest energy level in the Cu  $d$  splitting due to interaction with the field of Ligand (O). This shows that Cu is surrounded by O atom in tetragonal symmetry instead of square planar. The possible explanation of the result is that the CuO in a complex crystal can be inclined in slightly tetragonal symmetry through the coordination of Cu with six O atoms ligand around it, even though two of O atom not directly bonded. But this conclusion needs to be clarified further, since the previous calculation obtained different results.

Next we applied GW approximation for calculating electronic properties of CuO. In many body systems, screening effect occurs when electrons within the lattice of positive ions will repel each other, so that the area will be formed around the electron is called a screening hole, thus Coulomb interaction between electrons is reduced compared to vacuum conditions. This gave rise to the concept of quasi-particles ‘QP’ (electrons plus their screening hole). Interactions between electrons in many body systems can be replaced by a weaker interaction between quasi particles. So that, GW approximation uses QP approach, instead of electrons. GW approximation used here is a non-scf GW ( $G_0W_0$ ). A  $G_0W_0$  calculation is performed on the top of DFT where the electron wave functions are obtained from self-consistent DFT is used as a reference for the calculation of QP self-energy and energy correction to DFT.

Without U, GW approximation is able to open the band gap of up to 0.76 as shown in figure 5 (a). Screening done by GW has been effective to shift the band gap, in this case we used RPA (random-phase approximation), even though the band gap are still narrow. With perform GW calculation on the top of DFT+U, the obtained band gap can be set by adjusting the value of U. Like the DFT+U, the band gap of GW also increases linearly with U values. At  $U = 0.35$ , the band gap is very close to the experimental data, about 1.69 eV as shown in Table 1, and at  $U = 1.0$ , the band gap is overestimate, about 3.24 eV as shown in figure 5(b). In addition, the GW calculation has changed the band gap characteristics of CuO from indirect to direct bandgap.

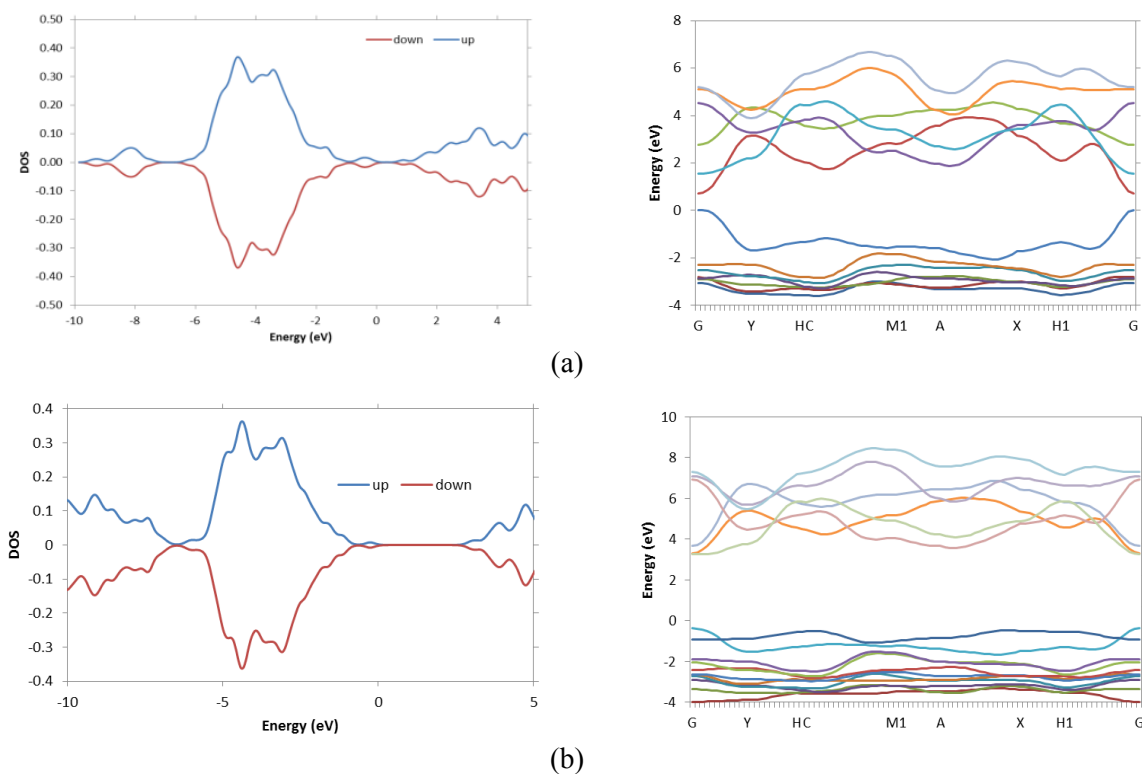


**Figure 5.** Total DOS and band structure of CuO calculated with  $G_0W_0$  on top of DFT+U,  $U = 0$  eV (a), and  $U = 1$  eV (b).

### 3.2. Optical Properties

Optical spectroscopy provides detailed information of the electronic structure of material. The optical properties of CuO have been studied experimentally [13]. Here we calculated optical properties of CuO based on DFT+U and GW correction by solving Bethe-Salpeter equation through Yambo package. Based on calculated dispersive part of dielectric function  $\epsilon_1(\omega)$  and the absorptive part  $\epsilon_2(\omega)$ , then we calculate the refractive index  $n$  and the extinction coefficient  $k$  through the relation in equation (1) as follows [13].

$$n = \sqrt{\frac{1}{2} \left( \sqrt{\epsilon_1^2 + \epsilon_2^2} + \epsilon_1 \right)},$$

$$k = \sqrt{\frac{1}{2} \left( \sqrt{\epsilon_1^2 + \epsilon_2^2} - \epsilon_1 \right)}.$$
(1)

Figure 6(a) shows the calculated of the imaginary part  $\epsilon_2(\omega)$  compared to the experimental result. The calculated electronic structure for varying  $U$  reflected in the dielectric function  $\epsilon_2(\omega)$ , the greater  $U$  the curve of  $\epsilon_2(\omega)$  shifted to the right. Direct band gap shown by the knee (kink) of  $\epsilon_2(\omega)$ , For  $U = 2.0$  we found kink around 1.0 eV, for  $U = 3$  kink around 1.4, while for  $U = 4$  kink around 1.7, this result closely to the previous result. Computed static electronic dielectric constant  $\epsilon(\infty) = \text{Re}(\epsilon(0))$  for varying  $U$  are 4.5, 5.4, and 6.8 for  $U = 2, 3, 4$ , respectively (see figure 6(b)). Ekuma et al [5] reported a value of 6.12 and Lany [6] reported a value 7.9. In figure 6(c, d) we shows the calculated refractive index  $n$  and the extinction coefficient  $k$  in good agreement with experimental data.

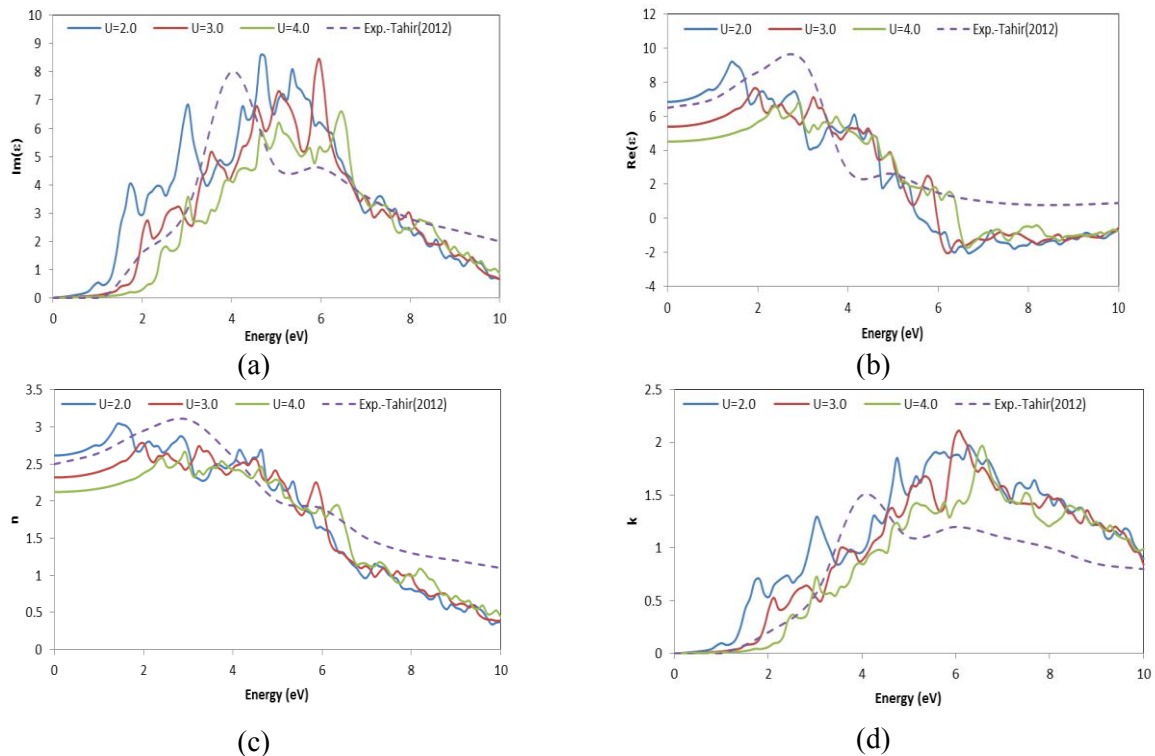


**Figure 6.** Calculated optical properties of CuO for varying  $U$  compared to experimental data [13], dielectric function  $\epsilon_1(\omega)$  (a),  $\epsilon_2(\omega)$  (b), refraction index  $n$  (c), and extinction coefficient  $k$  (d).

#### 4. Conclusions

We have performed DFT+U and GW approximation to study the electronic and optical properties of tenorite (CuO). Our calculation shows that DFT+U and GW approximation sufficiently reliable to investigate the material properties of CuO. The calculated band gap of DFT+U for reasonable value of U slightly underestimates. The use of GW approximation requires adjustment of U value to get realistic result. Hybridization Cu  $3d_{xz}$ ,  $3d_{yz}$  with O  $2p$  plays an important role in the formation of CuO bandgap. The calculated optical properties are in good agreement with experiment.

#### Acknowledgments

We acknowledge the support of Laboratory of Theoretical Physics IPB and GRID LIPI for high performance computing resources. F Ahmad wishes to thank Directorate General of Human Resource for Science, Technology and Higher Education, Indonesia for BPDN scholarship for this study.

#### References

- [1] Kum J M, Yoo S H, Ali G and Cho S O 2013 *Int. J. Hydrogen Energy* **38**, 13541–13546.
- [2] Zhang Q, Zhang K, Xua D, Yang G, Huang H, Nie F, Liu C and Yang S 2014 *Prog. Mater. Sci.* **60**, 208–337.
- [3] Claudia R, Sottile F and Reining L 2015 *Phys. Rev. B* **91**, 045102.
- [4] Wu D and Zhang Q 2006 *Phys. Rev. B* **73**, 235206.
- [5] Ekuma C E, Anisimov V I, Moreno J, and Jarrell M 2014 *Eur. Phys. J. B* **87**: 23.
- [6] Lany S 2013 *Phys. Rev. B* **87**, 085112.
- [7] Giannozzi P, *et al.* 2009 *J. Phys. Condens. Matter* **21**, 395502.
- [8] Marini A, Hogan C, Grüning M and Varsano D 2009 *Comput. Phys. Commun.* **180**, 1392–1403.
- [9] Forsyth J B and Hull S 1991 *J. Phys. Condens. Matter* **3**, 5257–5261.
- [10] Forsyth J B, Brown P J and Wanklyn B M 1998 *J. Phys. C Solid State Phys.* **21**, 2917–2929.
- [11] Yang B X, Thurston T R, Tranquada J M and Shirane G 1989 *Phys. Rev. B* **39**, 4343–4349.
- [12] Marabelli F, Parravicini G B and Salghetti-Drioli F 1995 *Phys. Rev. B* **52**, 1433–1436.
- [13] Tahir D and Tougaard S 2012 *J. Phys. Condens. Matter* **24**, 175002.